Indian Journal of Science and Technology, *Vol 9(24), DOI: 10.17485/ijst/2016/v9i24/95173, June 2016*
ISSN (Print) : 0974-6846
ISSN (Online) : 0974-5645

GCMT- 249 Investigation and Performance Analysis of Direct Torque Control of 3ϕ Induction Motor using 7 Level Neutral Point Clamped Multilevel Inverter

S. Priya[1*], A. Suresh[1] and M. R. Rashmi[2]

[1] Department of Electrical and Electrical Engineering, S. A. Engineering College, Chennai-600054, Tamil Nadu, India; priyasakthikumar@gmail.com, asuresz@gmail.com

[2] Amita Vishwa Vidyapeetham, School of Egineering, Bangalore-560055, Karnataka, India; rashmi.power@gmail.com

Abstract

Objective: This work discusses with Direct Torque Control (DTC) of Induction motor using 7 Level NPC Multilevel inverter for reducing the complexity in conventional DTC method. **Methods:** The limitation of traditional DTC scheme is more distortion in torque profile and the mean torque output never meets the torque demand. To get better performance of the traditional DTC a Space Vector Modulation (SVM) technique is projected to meet the torque and flux demands at low speeds. **Findings:** By designing 7 level NPC for DTC of induction motor and thereby simplifying the classical DTC method and in very particular this paper is minimizing the complications in Torque and Flux control at minimal speeds by decoupling the torque and flux controls and also reduces the ripples in current and torque profile. 7 level NPC is introduced in this paper which helps in eliminating the torque disturbances into minimum. The proposed 7 level inverter uses less number of switches and neutral-point fluctuations are absent in this model. Detached DC supplies are employed for the DC links which carries the ripple current. The proposed inverter topology provided the required magnitudes and phases of voltage and current vectors to meet the desired load values with fewer harmonic content due to superior level inverter and less distortion in torque profile obtained in the closed loop DTC technique.[1] The DTC of Induction Motor simulated by implementing the SVM technique using 7 level NPC and the simulation results are experimentally validated.**Improvements:** The steady state torque and speed output have less ripple content which reduces the oscillation with a quick response at steady state was investigated.

Keywords: Direct Self Control (DSC), Direct Torque Control (DTC), Multilevel Level Inverter (MLI), Neutral Point Clamped(NPC), Space Vector Modulation (SVM)

1. Introduction

To obtain adequate control of 3ϕ squirrel cage induction motor speed, torque, current, and magnetic flux, the multifaceted electronic controllers and converters are necessary. The H-Bridge MLI provides us a well improved output voltage profile when compared with established inverters[1]. Still to enhance the accomplishment of the H-Bridges , the quantity of voltage levels can be exploited when we use unbalanced power sources scaled in power of three[2]. The Total Harmonic Distortion (THD) is reduced due to increase in the quantity of voltage levels which in turn cut down rapid changes in V and I of common mode, minimised switching losses with absence of filters[3]. Since Switching losses are reduced so it operates at very low frequency for asymmetrical power sources[4].

The traditional methods like FOC use coordinate transformation and PWM signals generator unlike DTC does not requires current regulators steer to simplicity in design for controlling the incuction motor[5]. The earlier transducers are avoided by using DTC or DSC to acquire a good robust torque control.The inverter operating with low switching frequency use the basic schemes of DSC in the high power range applications that substantiate higher current distortion[6].

**Author for correspondence*

The bidirectional afloat power sources and the deficient of modularity problems in asymmetric multilevel inverters are lessened in DTC of drives which make use of three level diode clamped or neutral point clamped inverters[7–10]. A new switching sequence was introduced to balance the neutral-point voltage[11].

2. Direct Torque Control (DTC) Scheme

In vector controlled drives Direct torque and flux control technique is introduced which is an advanced scalar control for voltage source PWM inverter drives and ensures the enhanced performance. The developed electro magnetic torque is represented as

$$\overline{T_e} = \frac{3}{2}\left(\frac{P}{2}\right) \overline{\Psi_s} \text{ X } \overline{I_s} \tag{1}$$

where, $\overline{\psi_s} = \psi_{qs}{}^s - j\psi_{ds}{}^s$ and $\overline{I_s} = I_{qs}{}^s - jI_{ds}{}^s$

The $\overline{\psi_s}$ and $\overline{\psi_r}$ can be expressed as

$$\overline{\psi_s} = L_s\overline{I_s} + L_m\overline{I_r} \tag{2}$$

$$\overline{\psi_r} = L_r\overline{I_r} + L_m\overline{I_s} \tag{3}$$

From Equation (3)

$$\overline{I_r} = \frac{\overline{\psi_r} - L_m\overline{I_s}}{L_r} \tag{4}$$

Substituting Equation (4) in (2)

$$\overline{\psi_s} = L_s\overline{I_s} + L_m\left(\frac{\overline{\psi_r} - L_m\overline{I_s}}{L_r}\right)$$

Simplifying further

$$\overline{\psi_s} = \frac{L_m}{L_r}\overline{\psi_r} + \left(L_s + \frac{L_m{}^2}{L_r}\right)\overline{I_s} \tag{5}$$

$$\overline{I_s} = \frac{\psi_s - \frac{L_m}{L_r}\overline{\psi_r}}{L_s + \frac{L_m{}^2}{L_r}} \tag{6}$$

Therefore Equation (1) is rewritten as

$$\overline{T_e} = \frac{3}{2}\left(\frac{P}{2}\right)\frac{\frac{L_m}{L_r}\overline{\psi_r}}{L_s + \frac{L_m{}^2}{L_r}} \text{X}\overline{\psi_s} \tag{7}$$

The scalar value of torque is given by

$$\overline{T_e} = \frac{3}{2}\left(\frac{P}{2}\right)\frac{\frac{L_m}{L_r}}{L_s + \frac{L_m{}^2}{L_r}}|\psi_r||\psi_s|\sin\gamma \tag{8}$$

the torque angle between the fluxes is denoted as γ. The phasor diagram is represented in Figure 1 and this clearly demonstrates that the rotor flux does not show any change but the stator flux is changed for every small change in

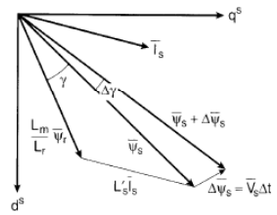

Figure 1. Phasor diagram.

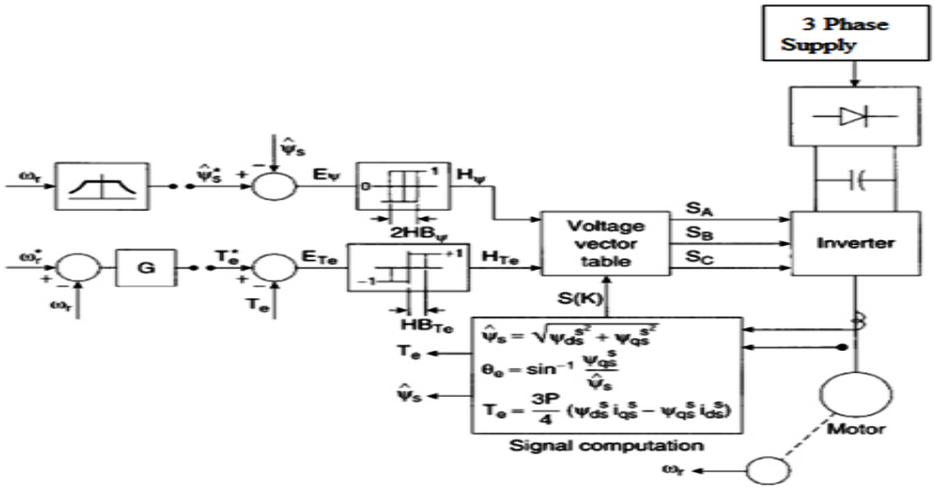

Figure 2. Block diagram representation of DTC.

stator voltage, and also the change of angle is γ is $\Delta\gamma$, the change in torque ΔT_e is represented by expression (9).

$$\overline{\Delta T_e} = \frac{3}{2}\left(\frac{P}{2}\right)\frac{\frac{L_m}{L_r}}{L_s + \frac{L_m}{L_r}^2}\left|\psi_r\right|\left|\overline{\psi_s} + \Delta\overline{\psi_s}\right|\sin\Delta\gamma$$

The block diagram is represented in Figure 2 and the control approach is exposed in Figure 3. The authentic values of ψ_s and T_e calculated from induction motor match with their set values and the results from the comparator block given to hysteresis band controllers[13]. The controller which process the flux value has two digital outputs based on the two equations given below:

$$H_\psi = 1 \text{ for } E_\psi > +HB_\psi \tag{10}$$

$$H_\psi = -1 \text{ for } E_\psi < -HB_\psi \tag{11}$$

where, $2HB_\psi$ is the band width of the flux controller. Figure 3(a) represent the anticlockwise rotation of the reference $\overline{\psi_s}$ with the hysteresis band. The actual $\overline{\psi_s}$ follows the command flux in a zigzag path and is forced within the hysteresis band. The 3 levels of digital output for torque control loop have the following relations:

$$H_{Te} = 1 \text{ for } E_{Te} > +HB_{Te} \tag{12}$$

$$H_{Te} = -1 \text{ for } E_{Te} < -HB_{Te} \tag{13}$$

$$H_{Te} = 0 \text{ for } -HB_{Te} < E_{Te} < +HB_{Te} \tag{14}$$

The machine line voltages and currents are utilised for estimating the feedback flux and torque. The segment number *S(k)* is deliberated from the signal computation block which in turn helps us to find the flux vector ψ_s position. In Figure 3(a) six sectors each of 60^0 angle wide is designated[e]. As per the voltage switching table exposed in Table 1 the voltage vector table block takes the input signals H_ψ, H_{Te} and *S(k)* and generates the appropriate control voltage vector switching states for the inverter[12].

The six active and two inactive inverter voltage vectors and a typical $\overline{\psi_s}$ are shown in Figure 3(b)[12]. The V_s is characterized by the subsequent eqation without tackig the stator resistance R_s of the motor,

$$\overline{V_s} = \frac{d}{dt}\left(\overline{\psi_s}\right) \tag{15}$$

Or

$$\Delta\overline{\psi_s} = \overline{V_s}.\ \Delta t \tag{16}$$

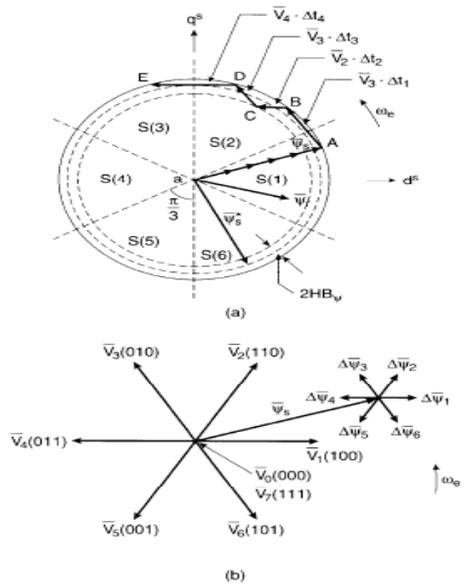

Figure 3. (a) Circular Trajectory of stator flux (b) MLI voltage vectors and equivalent changes of ψ in Δ*t*.

which implies that for every change in time Δt, $\overline{\psi_s}$ can be changed which is measured using stator voltage vector $\overline{V_s}$. Figure 3(b) represents the $\Delta\overline{\psi_s}$ corresponding to each inverter voltage vectors. Primarily the flux in the induction motor is recognized at zero frequency which lies on the radial trajectory OA and is exposed in Figure 3(a). The stator flux linkage $\overline{\psi_s}$ commences to revolve when the command torque is imposed along with the rated flux. Table 1 pertains the particular voltage vector, which fundamentally influences the T_e and $\overline{\psi_s}$ concurrently. The $\overline{\psi_s}$ sectors *AB, BC, CD* and *DE* by the individual voltage vectors $\overline{V_3}$, $\overline{V_4}$, $\overline{V_3}$ and $\overline{V_4}$ are shown in Figure 3(a)[12]. Because of the large value of T_r the $\overline{\psi_r}$ variation is very slow but $\overline{\psi_s}$ the Vs varies rapidly by $\overline{V_s}$. *For* ω_e, the $\overline{\psi_r}$ is more filtered and it travals consistently, while ψ_s movement is erratic. Under steady state operation the normal speed of ψ_s and $\overline{\psi_r}$ maintains the equal. Table 2 recapitulates the toque and flux values and direction for $\overline{\psi_s}$ as per the Figure 3(b)[12].

The $\overline{\psi_s}$ can be augmented by the $\overline{V_1}$, $\overline{V_2}$ and $\overline{V_6}$, whereas the same can be reduced by $\overline{V_3}$, $\overline{V_4}$ and $\overline{V_5}$. Similarly, T_e augmented by $\overline{V_2}$, $\overline{V_3}$ and $\overline{V_4}$, whereas it can bet diminished by $\overline{V_1}$, $\overline{V_5}$ and $\overline{V_6}$. The nil vectors V_0 or V_7 short circuits the load side and leave the $\overline{\psi_s}$ and T_e unaffected. Because of predetermined R_s drop, the $\overline{\psi_s}$ and T_e will somewhat lessen during the short circuit condition. The machine can effortlessly activate in all four

Table 1. Switching table

H_ψ	H_{Te}	$S(1)$	$S(2)$	$S(3)$	$S(4)$	$S(5)$	$S(6)$
1	1	V_2	V_3	V_4	V_5	V_6	V_1
	0	V_0	V_7	V_0	V_7	V_0	V_7
	-1	V_6	V_1	V_2	V_3	V_4	V_5
-1	1	V_3	V_4	V_5	V_6	V_1	V_2
	0	V_7	V_0	V_7	V_0	V_7	V_0
	-1	V_5	V_6	V_1	V_2	V_3	V_4

Table 2. ψ_s and T_e changes

Voltage Vector	V_1	V_2	V_3	V_4	V_5	V_6	V_0 or V_7
ψ_s	↑	↑	↓	↓	↓	↑	0
T_e	↓	↑	↑	↑	↓	↓	↓

quadrants, and speed loop and flux deteriorating control can be additionaly included. The switching frequency is not constant due to hysteresis controllers.

3. Neutral Point Clamped (NPC) Multilevel Level Inverter (MLI) for DTC

Figure 4 illustrates the block diagram of the proposed scheme[10]. The 7 level NPC multilevel inverter constructs the essential Voltage and current vectors to oblige Induction Motor[3]. The Torque and Flux calculator which is actually a hysteresis controller evaluate values produced by the 7 level NPC[13]. The vector divergence of current vectors produced by NPC induces the third current vector. By contrasting ω_r with the ω^*_r the speed controller produces the T^*_e and λ^*_S.

To calculate electromagnetic torque, stator flux linkages and stator currents are taken into account by using PI controller and steps are computed[14]. The dependency on motor parameters is reduced. For calculating stator flux linkages, stator resistance is measured which eradicate the needs of mutual and rotor inductances of the induction motor.

It also produces the V^*_d and V^*_q in 'd-q' plane.Then V^*_a, V^*_b, and V^*_c are matched with the appropriate carrier signal to engender proper PWM signals for the switching of the NPC MLI switches. Then the NPC MLI produces the necessary V_a, V_b and V_c and I_a, I_b and I_c of proper values to satisfy the needed load values with diminished harmonics due to 7 level NPC MLI which inturn produces better torque profile with lessen ripples[15].

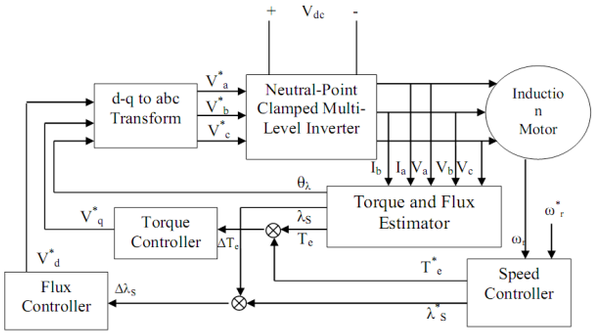

Figure 4. Proposed system.

4. Simulation Results

The projected 7-Level NPC Multilevel Inverter is revealed in Figure 5 and the closed loop simulation of the 7-Level NPC Inverter with the DTC of induction drive is exposed in the Figure 6. The 3ϕ induction drive parameters are specified in Table 3.

Figures 7 and 8 illustrate the output phase and line voltage of each leg of the 7 Level NPC MLI. Rotor and stator current waveforms are pointed up in Figures 9 and 10, correspondingly. Figures 11 and 12 exhibit the Torque and speed profile of the 3ϕ induction drive.

From the above results, it can be inferred that the DTC implementation for the 3φ Induction Motor by means of the 7 Level NPC MLI would provide the leg voltage waveform of seven-levels with THD reaching zero at 0.008 seconds with slight distortion in the range of 0.01 to 0.03 seconds. This also provides a steady state torque output at 0.166 seconds after a peak overshoot of 82 Nm. The Steady state Torque Output has ripple causing variation within a range of 7Nm. The speed also has ripple contents that causes it to oscillate within a range of 25 rpm at Steady state.

5. Experimental Validation of Seven Level NPC For DTC Of Induction Motor

The hardware setup for 7-Level NPC MLI is exposed in Figure 13. This prototype consist of seven level inverter circuit, driver circuit for NPC, control unit, Speed sensing circuit, power supply unit and induction motor along with loading arrangement. The seven level output voltage represented in Figure 14 and inferred that the output voltage is nearly sinusoidal. The phase voltage output of seven level NPC captured in DSO which is shown in Figure 15.

Table 3. Induction motor parameter

Parameters	Rating
Three Phase	50Hz,4 kW, 400 V, 155 rad/s
Poles Pairs	2
Hp	5
Stator Rs and Rotor resistances Rr	Rs= 0.5ohms, Rr = 0.25 ohms
Stator Ls and rotor Lr self inductances	Ls = 0.0415; Lr = 0.0412 H
Mutual Inductance between stator and rotor Lm	Lm = 0.0403 H

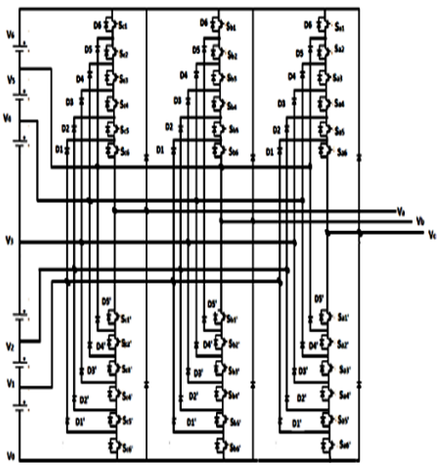

Figure 5. 7 level NPC multilevel inverter.

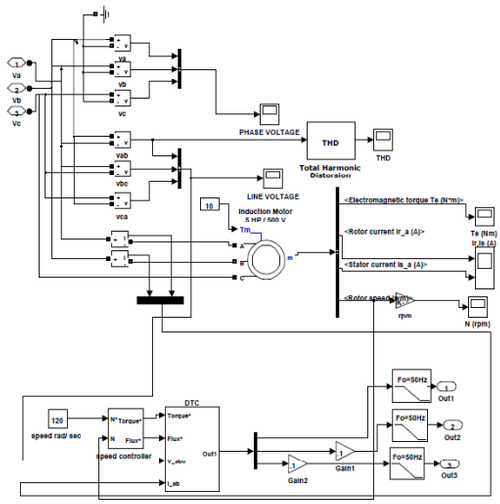

Figure 6. 7-level NPC inverter with DTC.

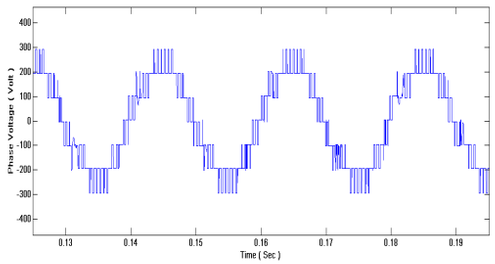

Figure 7. Phase voltage of the 7 level NPC.

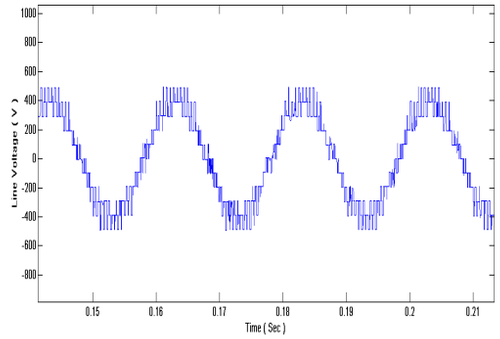

Figure 8. Line voltage of the 7 level NPC.

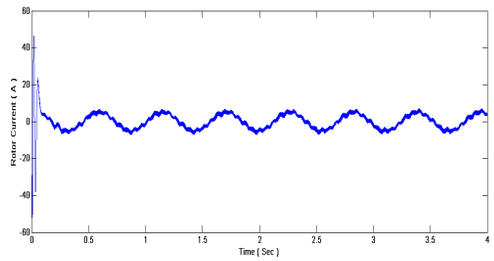

Figure 9. Rotor current waveform induction motor.

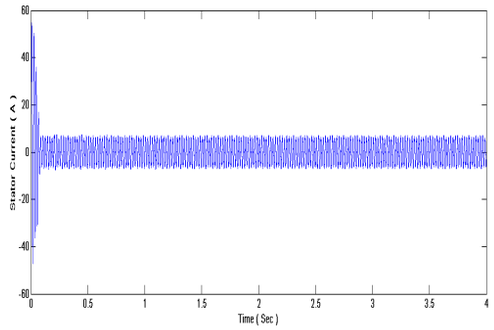

Figure 10. Stator current waveform of the induction motor.

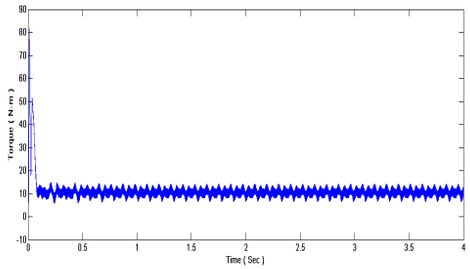

Figure 11. Motor torque output.

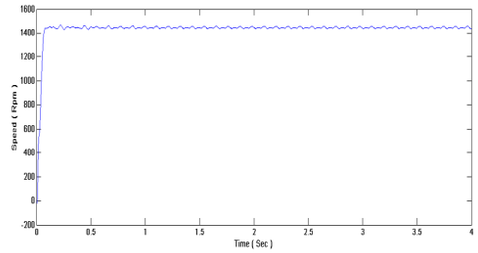

Figure 12. Speed output.

Figure 13. The hardware setup for seven-level NPC inverter.

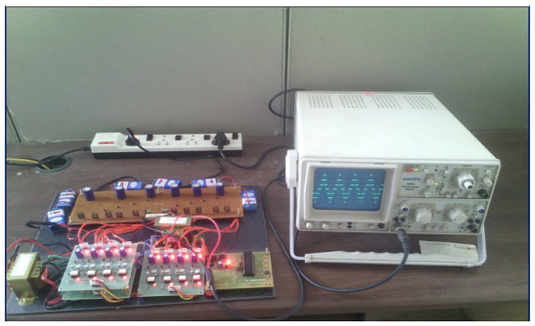

Figure 14. The seven level output voltage of NPC Inverter.

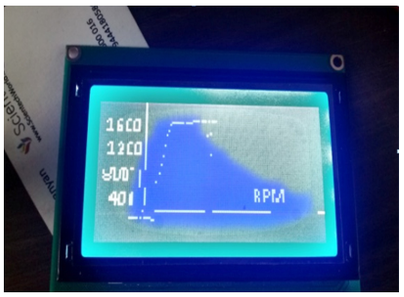

Figure 15. The speed output display of induction motor in graphical LCD.

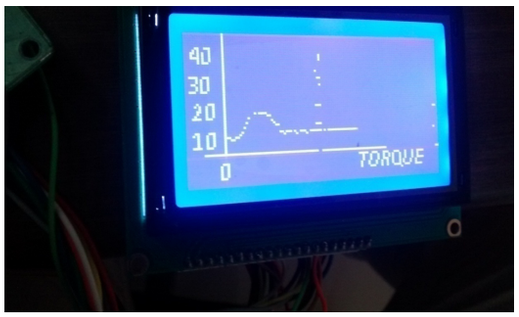

Figure 16. The Torque output display of induction motor in graphical LCD.

Table 4. Performance of induction motor drive with 7 level diode clamped inverter

Parameters	Simulation output	Hardware output
Output voltage level	7	7
Torque	10.1 nm	9.9 nm
Speed	1440 rpm	1480 rpm

The seven level phase output voltage shown in Figure 7 match with the simulation output and this output voltage is given to the induction drive. The speed and torque output of induction motor provided from 7-Level NPC MLI with Direct Torque Control are shown in Figures 15 and 16 with graphical LCD. The speed and torque simulation output taken with the Matlab/ simulink model which is experimentally validated with help of hardware Setup and comparison of hardware results with simulation results are publicized in Table 4.

6. Conclusion

The Design of 7 Level NPC MLI for the DTC of Induction drive was simulated by applying the DTC. From the simulated torque profile it is studied that the variations in the torque pofile are lessened in the projected system

compared to traditional system. The simulation results are experimentally authenticated and experimental results are in-line with simulation results.

7. References

1. Lai J-S, Zheng PF. Multilevel converters-a new breed of power converters., IEEE Transactions on Industry Applications. 1996 May; 32(3):509–17.
2. Dixon J, Moran L. Multilevel inverter, based on multi-stage connection of three-level converters scaled in power of three. Proceeding of 28th Annual Conference of the Industrial Electronics Society; 2002. p. 886–91.
3. Jain M, Sing A, Singh S. Comparative analysis and simulation of diode clamped & cascaded h-bridge multilevel inverter using SPWM Technique. International Journal of Engineering Research and Applications. 2015; 5(1): 95–102.
4. Leonhard W. Control of electrical drives. Springler-Verlag; 1990.
5. Takahashi I, Noguchi T. A new quick-response and high-efficiency control strategy of an induction motor. IEEE Transactions on Industry Applications. 1986; 22(5):820–7,
6. Depenbrock M. Direct Self-Control (DSC) of inverter-fed induction machine. IEEE Transactions Power Electronics. 1988; 3(4):420–29,
7. Kouro S, Bernal R, Miranda H, Rodriguez J, Pont J. Direct torque control with reduced switching losses for asymmetric multilevel inverter fed induction motor drives. Industry Applications Conference 41st IAS Annual Meeting Conference Record; 2006. p. 2441–46.
8. Brando G, Rizzo H. An optimized algorithm for torque oscillation reduction in DTC induction motor drives using 3-level NPC inverter. Proceedings IEEE International Symposium on Industrial Electronics. 2004; p. 1215–20.
9. Choi U-M, Lee J-S, Kyo-Beum. New modulation strategy to balance the neutral-point voltage for three-level neutral-clamped inverter systems. IEEE Transactions On Energy Conversion. 2014; 29(1):1–10.
10. Priya S, Rashmi MR, Suresh A. A novel scheme for reduction of torque ripple in direct torque control of three phase squirrel cage induction motor using seven level neutral point clamped inverter. Research Journal of Applied Sciences, Engineering and Technology. 2013; 5(5):1769–73.
11. Monge BS, Alepuz S, Bordonau J, Peracaula J. Voltage balancing control of diode-clamped multilevel converters with passive front-ends. IEEE Transactions Power Electron. 2008; 23(4):1751–58.
12. Sahu MK, Panigrahi BP, Panda AK. An utility friendly direct torque control technique of three phase induction motor with two level inverter using 180 degree conduction mode. International Journal of Engineering Science and Technology. 2011; 3(5):4120–30.
13. Manjula HS, Sasikumar M. Current harmonics reduction using Hysteresis Current Controller (HCC) for a wind driven self-excited induction generator drives. Indian Journal of Science and Technology. 2015; 8(13):1–6. DOI: 10.17485/ijst/2015/v8i13/60330.
14. Sahu SK, Dixit TV, Neema DD. Indirect vector control of multilevel inverter fed induction motor using ANN estimator and ANFIS controller. Journal of Electrical Engineering. 2015; 15(1):1–6.